Check for updates

Society For
Biomaterials

| RESEARCH ARTICLE | OPEN ACCESS

Enhanced Metabolic Syndrome Management Through Cannabidiol-Loaded PLGA Nanoparticles: Development and In Vitro Evaluation

Mazen M. El-Hammadi[1] 🄳 | Lucía Martín-Navarro[1] | Esther Berrocoso[2,3,4] | Josefa Álvarez-Fuentes[1,5] |
Benedicto Crespo-Facorro[2,5,6] | Irene Suárez-Pereira[2,4,7] | Javier Vázquez-Bourgon[2,8,9] | Lucía Martín-Banderas[1,5] 🄳

[1]Department of Pharmacy and Pharmaceutical Technology, Faculty of Pharmacy, Universidad de Sevilla, Sevilla, Spain | [2]Centro de Investigación Biomédica en Red en Salud Mental (CIBERSAM), Madrid, Spain | [3]Neuropsychopharmacology & Psychobiology Research Group, Department of Psychology, University of Cadiz, Cádiz, Spain | [4]Biomedical Research and Innovation Institute of Cádiz (INiBICA) Research Unit, Puerta del Mar University Hospital, University of Cádiz, Cádiz, Spain | [5]Instituto de Biomedicina de Sevilla (IBIS)-Campus Hospital Universitario Virgen del Rocío, Sevilla, Spain | [6]Department of Psychiatry, School of Medicine, University Hospital Virgen del Rocio, Sevilla, Spain | [7]Neuropsychopharmacology & Psychobiology Research Group, Department of Neuroscience, University of Cadiz, Cádiz, Spain | [8]Department of Psychiatry, University Hospital Marqués de Valdecilla. Instituto de Investigación Sanitaria Valdecilla (IDIVAL), Santander, Spain | [9]Departamento de Medicina y Psiquiatría, Universidad de Cantabria, Santander, Spain

Correspondence: Mazen M. El-Hammadi (mazenhammadi@us.es) | Lucía Martín-Banderas (luciamartin@us.es)

ABSTRACT

Cannabidiol (CBD) holds promise for managing metabolic diseases, yet enhancing its oral bioavailability and efficacy remains challenging. To address this, we developed polymeric nanoparticles (NPs), using poly(lactic-co-glycolic acid) (PLGA), encapsulating CBD using nanoprecipitation, aiming to create an effective CBD-nanoformulation for metabolic disorder treatment. These NPs (135–265 nm) demonstrated high encapsulation efficiency (EE% ≈ 100%) and sustained release kinetics. Their therapeutic potential was evaluated in an in vitro metabolic syndrome model employing sodium palmitate-induced HepG2 cells. Key assessment parameters included cell viability (MTT assay), glucose uptake, lipid accumulation (Oil Red O staining), triglycerides, cholesterol, HDL-c levels, and gene expression of metabolic regulators. Results showed an IC50 of 9.85 μg/mL for free CBD

------

and 11.26 μg/mL for CBD-loaded NPs. CBD-loaded NPs significantly enhanced glucose uptake, reduced lipid content, lowered triglycerides and total cholesterol, and increased HDL-c levels compared to free CBD. Gene analysis indicated reduced gluconeogenesis via downregulation of PPARγ, FOXO-1, PEPCK, and G6Pase and enhanced fatty acid oxidation through CPT-1 upregulation. These findings suggest that CBD-loaded NPs may serve as a novel therapeutic strategy for the management of metabolic disorders, warranting further in vivo studies.

1 | Introduction

The exposure to antipsychotic medication has been widely associated with weight gain and lipid/glucose metabolic side effects of clinical relevance and, in some instances, the development of metabolic syndrome [1–3]. At the same time, cannabis use is significantly more frequent among individuals with psychosis than in the general population [4, 5]. Despite being one of the main risk factors for psychosis [6] and its widely described deleterious effect on psychosis' prognosis [7–11], recent research has shown a protective effect of cannabis on antipsychotic-induced weight gain [12, 13]. These studies have also suggested a protective effect against the lipid metabolic disorders typically associated with weight gain in this population [14, 15]. Additionally, cannabis has been linked to a positive effect on glucose metabolism, correlating with reduced levels of fasting insulin and HOMA-IR [16] and lower prevalence of diabetes mellitus [17, 18].

This protective effect may be explained by the interaction between consumed cannabis and the endocannabinoid system, which influences both eating patterns and the storage and utilization of peripheral energy [19–25].

Cannabis comprises a diverse array of phytocannabinoids, among which cannabidiol (CBD), non-psychoactive, stands out as a primary component. It is known for its pain-relieving, anti-inflammatory, anti-oxidant, anti-tumor, and neuroprotective properties [26–28]. Several studies have highlighted CBD's influence on both lipid and glucose metabolism, mediated through various receptors and metabolites reducing the risk of developing metabolic syndrome [29–31]. Furthermore, CBD acts as a serotonin receptor antagonist, potentially alleviating hyperphagia [32]. While CBD exhibits a low affinity for CB1 and CB2 receptors, it can antagonize these receptors at nanomolar range [33], suggesting CBD's ability to interact with them at relatively low concentrations.

Several studies have evaluated the impact of CBD and other cannabinoids on lipid metabolic disorders, suggesting potential beneficial effects through the modulation of the endocannabinoid system (ECS). CBD has been reported to reduce lipid accumulation in hepatocytes and adipocytes, improve insulin sensitivity, and modulate the expression of genes related to lipogenesis and β-oxidation [34, 35]. At the molecular level, CBD acts on receptors such as PPARγ, AMPK, and TRPV1, influencing key metabolic pathways associated with lipid homeostasis [31]. However, the use of cannabinoids in these contexts is not without adverse effects. Hepatic alterations, changes in blood pressure, and potential psychoactive effects have been reported, depending on the dosage and formulation used [36]. These findings highlight the need for further studies to determine the long-term safety and efficacy profile of these therapies in the treatment of metabolic disorders.

Recent studies suggest that CBD may have certain toxic effects in living organisms, potentially due to its interactions with various biological targets. These include cannabinoid receptors (CB1 and CB2), transient receptor potential (TRP) channels, and cytochrome P450 (CYP450) enzymes. By modulating these systems, CBD can alter neurotransmitter release, calcium balance, and drug metabolism, which may contribute to risks such as hepatotoxicity and neurotoxicity. For example, CBD-induced inhibition of CYP450 enzymes, especially CYP3A4 and CYP2C19, can interfere with the metabolism of co-administered drugs, leading to elevated drug plasma concentrations and a higher risk of toxicity [36, 37]. In addition, prolonged activation of TRPV4 channels by CBD has been shown to cause cellular stress and even cell death in glioma cells [38]. While these highlight potential safety concerns, further research is necessary to fully understand the mechanisms underlying CBD's toxicological profile and its overall impact on human health.

Developing CBD as a therapeutic formulation faces challenges due to its high lipophilicity and poor oral bioavailability, estimated to be as low as 6% of a similar intravenously administered dose [39]. Traditional delivery strategies, such as oral administration, suffer from extensive first-pass metabolism, leading to reduced systemic availability and unpredictable pharmacokinetics [40]. Similarly, inhalation-based delivery, while offering rapid absorption, raises concerns regarding pulmonary irritation and inconsistent dosing [41]. Over the past decades, researchers have explored various nanocarriers, including liposomes, polymeric nanoparticles (NPs), micelles, dendrimers, and solid lipid nanoparticles (SLNs), for their potential in targeted drug delivery and controlled release [42–44]. Among these, poly(lactic-co-glycolic acid) (PLGA) NPs have gained particular attention due to their excellent biocompatibility, biodegradability, and versatility in encapsulating both hydrophilic and hydrophobic drugs [45, 46]. To further optimize the performance of these NPs, PEGylation, the process of conjugating polyethylene glycol (PEG) to NPs, enhances their physicochemical properties by improving solubility, reducing opsonization by the mononuclear phagocyte system (MPS), and prolonging systemic circulation time [47, 48]. These advancements are particularly relevant for delivering drugs to metabolically active organs like the liver, which plays a key role in conditions such as metabolic syndrome. Disorders like obesity, type 2 diabetes, and non-alcoholic fatty liver disease (NAFLD) are driven by complex molecular mechanisms. These include insulin resistance, chronic inflammation, oxidative stress, and imbalances in lipid metabolism [49–51]. Understanding and targeting these pathways with advanced

nanoformulations could pave the way for more effective therapeutic interventions.

In our previous studies, we demonstrated the successful encapsulation of cannabinoids, specifically Δ9-tetrahydrocannabinol and naphthalen-1-yl-(4-pentyloxynaphthalen-1-yl) methanone (CB13; a synthetic cannabinoid), within PLGA-based nanosystems. These nanosystems exhibited favorable biodistribution in vivo and were effective via the oral route [52–55].

In the present work, we have developed a PEGylated PLGA nanoformulation for CBD and carried out a deep study in an in vitro metabolic disease model in order to understand the intricate mechanisms through which cannabinoids influence hepatic functions as a key step for unraveling their therapeutic potential in metabolic syndrome [53–55].

To the best of our knowledge, no previous work has reported on the development of CBD-nanosystems for these therapeutic applications, assessing their capacity to enhance glucose uptake and prevent lipid accumulation in human HepG2 hepatocytes.

2 | Materials and Methods

2.1 | Materials

Poly(lactic-co-glycolic) acid block copolymer (PLGA 50:50) Resomer RG 502 (with an alkyl ester end group; Mw: 12000; inherent viscosity: 0.24 dL/g) was obtained from Evonik (Germany) and PEG-PLGA (PEG average Mn 2000, PLGA average Mn 11,500; lactide:glycolide 50:50) was purchased from Sigma-Aldrich (Germany). Synthetic CBD (Mile High Labs, Lot. IL1905027-A) was gently provided by GB Sciences (NV, USA). Pluronic F-68 and solvents were obtained from Panreac Química (Spain). Culture media, including minimum essential medium (MEM) and high glucose DMEM (Dulbecco's Modified Eagle Medium), were obtained from Corning (USA). All other chemicals were purchased from Merck (Germany). All chemicals were of analytical quality. Water used in the experiments was deionized and filtered (Milli-Q Academic, Millipore, Spain).

2.2 | Preparation of NPs

Nanoparticles were prepared using a nanoprecipitation method established by our research group [53–55]. Briefly, PLGA or PEG-PLGA (22.5 mg) and Span 60 (7.5 mg) were dissolved in acetone (1.5 mL). The organic phase was added to 9 mL Pluronic F-68 aqueous solution (0.5% w/v) using a syringe pump at a controlled rate of 5 mL/h accompanied by continuous stirring. The solvent was removed by stirring at room temperature, and the resulting nanoparticles were collected via ultrafiltration. The latter step involved transferring the NPs suspension into an Amicon tube (Ultracel-100 kDa regenerated cellulose membrane, 15 mL sample volume) and washing the nanoparticles with MQ water. The concentrated and purified NPs were recovered by centrifugation at 4000×g at 12°C. To generate CBD-loaded NPs, CBD was added at various ratios relative to the polymer weight (10%,

12.5%, and 15% w/w) to the organic phase. The concentrated NP suspension was collected and diluted with PBS to a final volume of 1 mL for further analysis.

2.3 | NPs Characterization

The NPs were characterized by measuring mean diameter and zeta potential using dynamic light scattering and laser Doppler electrophoresis (Nanosizer ZS, Malvern Instruments, UK). NP morphology was assessed using scanning electron microscopy (SEM) and transmission electron microscopy (TEM). For SEM, a drop of 1 mg/mL NP suspension was air-dried on a carbon strip and coated with an 8–9 nm Pd/Pt shell (Leica EM SCD500). Images were taken with a Zeiss Crossbeam 550 SEM (Carl Zeiss Microscopy, Germany). For TEM, a drop of NP suspension was placed on a copper grid, stained with 2% uranyl acetate, air-dried, and observed using a Zeiss Libra 120 TEM (Carl Zeiss Microscopy, Germany).

2.4 | Measurement of CBD Load Capacity

CBD loading into PLGA-based nanoparticles (NPs) was assessed using reverse phase-high performance liquid chromatography (RP-HPLC), previously validated for precision, accuracy, and linearity [56]. The analysis was performed on a Hitachi LaChrom1 HPLC system equipped with a C18 Waters Atlantis T3 column (3 μm, 4.6×100 mm) at 25.0°C±0.1°C. The mobile phase consisted of methanol, acetonitrile, and water (52:30:18 v/v) at pH 4.5, with a flow rate of 1 mL/min. Detection occurred at 210 nm with an injection volume of 10 μL. Data were analyzed using HSM D-7000 software. CBD standard solutions prepared in methanol showed a linear concentration-peak area relationship (Area $= 34{,}866 \times C + 272{,}704$; $R^2 = 0.9974$), and repeatability was indicated by a relative standard deviation (RSD) of 1.88%. Accuracy was confirmed with a mean recovery of 101.4% over a concentration range of 12.5–300 μg/mL, with an RSD of 1.90%. The analysis time was 10 min, yielding a sharp peak with a retention time of 4.4±0.4 min. The limit of detection (LOD) and limit of quantitation (LOQ) were determined as 5 and 6.25 mg/mL, respectively, following ICH guidelines. Encapsulation efficiency (EE%) and drug loading (DL%) were used to express the drug content.

$$EE\% = \frac{\text{total drug amount} - \text{unencapsulated drug amount}}{\text{total drug amount}} \times 100$$

(1)

$$DL\% = \frac{\text{total drug amount} - \text{unencapsulated drug amount}}{\text{total mass of NPs}} \times 100$$

(2)

In all subsequent experiments, CBD-loaded PLGA-PEG NPs, prepared with a CBD to polymer weight ratio of 15%, were utilized.

2.5 | In Vitro Release of CBD From Nanoparticles

In the in vitro CBD release study, PEG-PLGA NPs (2.5 mg/mL) loaded with CBD were dispersed in PBS (pH 7.4±0.1) containing

0.5% (w/v%) Tween 80 to maintain sink conditions. Samples were placed in a thermostatic shaker set at 37.0°C ± 0.5°C and subjected to mechanical stirring (500 rpm) (Titramax 1000, Heidolph, Germany). At selected time intervals (0.5–96 h), samples were centrifuged at 14,000 rpm for 20 min. The supernatant was removed, and the NP pellet was dissolved in acetonitrile. Drug release was calculated indirectly by measuring the amount of unreleased CBD remaining in the NPs using the HPLC method. Finally, the results were expressed as accumulative drug release percentages.

$$\%\text{Cumulative drug release} = \frac{\text{amount of drug loaded in NPs [mg]} - \text{amount of drug remained in NPs [mg]}}{\text{amount of drug loaded in NPs [mg]}} \times 100 \tag{3}$$

To quantitatively compare the drug release kinetics between PLGA and PEG-PLGA NPs, we calculated the difference factor (f_1) and similarity factor (f_2) as per FDA/EMA guidelines [57]. The f_1 (Equation 4) metric evaluates absolute differences between cumulative release profiles at each time point, while f_2 (Equation 5) assesses similarity through logarithmic transformation of squared errors. Reference (R) and test (T) profiles were defined as PLGA NPs and PEG-PLGA NPs, respectively. Calculations included all time points ($n = 13$), and thresholds of $f_1 < 15$ and $f_2 \geq 50$ were used to determine statistical similarity.

$$f1 = 100 \times \left(\frac{\sum_{t=1}^{n} |R_t - T_t|}{\sum_{t=1}^{n} R_t} \right) \tag{4}$$

$$f2 = 50 \times \log \left(100 \times \left[1 + \frac{1}{n} \sum_{t=1}^{n} (R_t - T_t)^2 \right]^{-0.5} \right) \tag{5}$$

where, n = number of time points; R_t = mean % drug released from PLGA NPs at time t after initiation of the study; T_t = mean % drug released from PEG-PLGA NPs at time t after initiation of the study.

2.6 | In Vitro Experiments

2.6.1 | Cell Maintenance

The HepG2 human hepatoma cell line (CLS, Germany) was cultured in minimum essential medium (MEM) supplemented with 10% fetal bovine serum and 1% penicillin/streptomycin. Cells were maintained at 37°C with 5% CO_2 in a humidified environment. Passage numbers 26–40 were used. Free CBD and metformin were initially dissolved in absolute ethanol (4 mg/mL) and PBS (5 mg/mL), respectively, before being further diluted in the culture media. Meanwhile, NP suspensions, including CBD-loaded and blank (drug-free) PEG-PLGA NPs, were directly dispersed and diluted in the media.

2.6.2 | Cell Viability Assay

Cell viability was assessed using the MTT assay. HepG2 cells (3×10^4 cells/well) were seeded in 96-well plates and incubated overnight at 37°C with 5% CO_2. Cells were treated with varying concentrations of free CBD and CBD-loaded PEG-PLGA NPs diluted in the media (0–50 μg/mL) for 24 h. Free CBD was first dissolved in absolute ethanol (4 mg/mL) then diluted in the Media. CBD NP suspension was also dispersed in the media for dilution. Cells were treated with varying concentrations of free CBD and CBD-loaded PEG-PLGA NPs (0–50 μg/mL) diluted in the culture media for 24 h. After treatment, 200 μL of MTT solution (0.5 mg/mL) was added and incubated for 4 h. The supernatant was removed, and formazan crystals were dissolved with 200 μL of DMSO. Untreated cells and Triton-x 1% treated cells were used as controls. Optical density at 570 nm was measured with a microplate reader (Synergy HT, BioTek Instruments Inc., Vermont USA). Relative cell viability (%) was calculated, and IC50 values were determined using GraphPad Prism 9.

2.6.3 | In Vitro Cell Model of Metabolic Syndrome

To investigate the effects of CBD on lipid metabolism and metabolic dysfunction, we employed HepG2 cells as an in vitro model of metabolic syndrome-like conditions. HepG2 cells have been extensively used to study hepatic lipid accumulation, insulin resistance, and oxidative stress, key features of metabolic syndrome [58, 59]. To induce a metabolic dysfunction state, cells were treated with a combination of high glucose (HG) and free fatty acids (FFA), specifically palmitic and oleic acids, as previously described [59, 60]. This approach mimics the pathophysiological conditions of hepatic steatosis and dyslipidemia observed in metabolic syndrome, providing a relevant platform to assess the impact of potential therapeutic agents on lipid metabolism [61, 62], as the PEGylated PLGA nanoplatforms developed in this work for the vehiculization of the CBD.

To assess glucose uptake, lipid accumulation, and the inflammatory profile in vitro, hepatic cells were incubated with sodium palmitate (PA) at a concentration of 0.35 mM simultaneously with the application of NPs. The concentration range of CBD formulations was selected to remain below the cytotoxic levels determined in the MTT assay.

2.6.3.1 | Glucose Uptake Assay.
Glucose uptake in HepG2 cells was measured using 2-NBDG (2-(N-(7-nitrobenz-2-oxa-1, 3-diazol-4-yl)amino)-2-deoxyglucose), with modifications from a previous method [63]. Cells (3×10^4 cells/well) were cultured in 96-black, clear bottom well plates (Corning Costar, USA) and incubated overnight at 37°C with 5% CO_2. Cells were then treated with free CBD, CBD-loaded PEG-PLGA NPs (0.25–5 μg/mL), or metformin (50 μg/mL) in high glucose DMEM (4500 mg/L) with 0.35 mM sodium palmitate for 24 h.

Control groups ethanol or blank NPs (drug-free PEG-PLGA NPs) were also treated with 0.35 mM sodium palmitate. After washing with PBS, cells were incubated in glucose-free DMEM for 3 h, followed by exposure to 50 μM 2-NBDG in glucose-free DMEM for 30 min. The reaction was terminated by washing with cold PBS, and fluorescence was measured using a microplate reader at 485 nm excitation and 535 nm emission.

2.6.3.2 | Oil Red O Staining.
Lipid droplet accumulation in HepG2 cells was assessed using the Oil Red O staining

method with modifications [64, 65]. HepG2 cells (5×10^5 cells/well) were cultured in 6-well plates and incubated overnight at 37°C with 5% CO_2. Cells were then treated with free or encapsulated CBD in the presence of 0.35 mM sodium palmitate (in serum-free MEM containing 1% BSA w/v fatty acid free) for 24 h. After removing the medium, cells were washed with PBS and fixed with 4% paraformaldehyde for 30 min. Cells were pre-incubated with 60% aqueous isopropanol for 5 min, then stained with 1.8 mg/mL Oil Red O in isopropanol for 15 min at room temperature, followed by PBS rinsing. After adding PBS, images were taken under an inverted microscope (Olympus CKX41, Olympus Corporation, Japan). For lipid quantification, Oil Red O was extracted with isopropanol, and 200 μL aliquots were transferred to a 96-well plate. Absorbance was measured at 490 nm using a microplate reader, with 3 samples per condition, each measured twice.

2.6.3.3 | Determining Levels of Medium HDL-c. HepG2 cells were treated with CBD in the presence of sodium palmitate, and the culture medium was collected to measure HDL cholesterol (HDL-c) levels. To quantify HDL-c, 100 μL of medium was mixed with precipitation buffer and incubated for 10 min. After centrifugation, low-density lipoprotein (LDL) and very low-density lipoprotein (VLDL) were precipitated. HDL-c in the supernatant was quantified using a reagent kit following the manufacturer's instructions (#MAK045, Merck, Germany). Three samples per condition were used, each measured twice.

2.6.3.4 | Determining Levels of Intracellular Triglyceride and Total Cholesterol. HepG2 cells used for HDL-c measurement were also employed to assess intracellular TG and cholesterol levels. After treatment with CBD and sodium palmitate, cells were washed with PBS, digested with trypsin (300 μL for 5 min), and suspended in medium (700 μL). Of the 1 mL suspension, 700 μL was used for lipid quantification. Cells were centrifuged at 500×g for 5 min, and lipids were extracted using hexane-isopropanol (v/v 3:2), followed by centrifugation at 13,000×g for 10 min at 4°C. The organic phase was dried, and cholesterol and TG levels were measured using Merck reagent kits (#MAK043 and #MAK266, Merck, Germany). Protein concentration was determined by lysing cells with a lysis buffer (1% Triton X-100 in PBS; 30 min), centrifuging (10,000×g for 10 min at 4°C), and using a BCA protein assay kit (#23227, Pierce-Thermo scientific, IL, USA). Lipid content was normalized to protein concentration. Three samples per condition were measured twice.

2.6.3.5 | Gene Expression Analysis. Total RNA was extracted from HepG2 cells, treated with PA, free CBD, or NPs as described above, using the High Pure RNA Isolation kit (Roche) following the manufacturer's procedure. Subsequently, cDNA was synthesized via reverse transcription-PCR (RT-PCR) using 1 μg of RNA samples using High-Capacity cDNA Reverse Transcription kit (Applied Biosystems) according to manufacturer's guidelines. Gene expression was analyzed by quantitative real-time PCR (qPCR) in the LightCycler 480 thermal cycler (Roche Diagnostic) using the PowerUp SYBR Green Master Mix (Applied Biosystems). Predesigned KiCqStart SYBR Green primers (KSPQ12012) used to make multiple copies of the genes related to glucose metabolism (*GLUT2*, *G6Pase*, and *PEPCK*), lipolysis (*CTP-1*), lipogenesis (*ACC-1*, *FAS-1*) and transcriptional

factors (*FOXO-1, SREB-1c, PPARγ* and *HNF4α*) were purchased from Sigma Aldrich. GAPDH was used as the reference gene. Data analysis was performed using LightCycler 480 Gene Scanning Software version 1.5 (Roche Diagnostic). Quantification cycle (Cq) values were acquired using the Second Derivative Maximum method. The expression profiles were calculated by the $2^{-\Delta\Delta Cq}$ method, normalized using the mean of the reference gene, and expressed as mRNA relative units [58, 66, 67]. Detailed primer sequences can be found in (Table S1).

2.7 | Statistical Analysis

Statistical analysis was conducted using the SPSS Statistics 26 statistical package (SPSS Inc., Chicago, IL). Data are presented as the mean ± standard deviation (SD). Experiments were designed to generate groups of equal size. The sample size '*n*' was defined as individual values for each experiment and that statistical analysis was performed using these independent values. All data obtained were used in the statistical analysis. Each experiment was independently replicated at least three times. Groups of two were analyzed with two-tailed (Student's) *t*-test, whereas comparisons involving more than two groups and a single variable were analyzed using one-way ANOVA analysis with LSD post hoc test, with $p < 0.05$ considered statistically significant.

3 | Results

3.1 | Nanoparticle Characteristics

The characteristics of the investigated NPs are outlined in Table 1. The mean diameter ranged from 135 to 270 nm with a narrow size distribution (PdI < 0.3) and a negative zeta potential. PEG-PLGA NPs exhibited the smallest particle size which, in agreement with previous findings [68], is thought to be attributed to the hydrophilic PEG coating that enhances the NPs' hydrophilicity and stability, resulting in smaller particles. Furthermore, PEG-PLGA NPs reported less negative zeta potential values (ranging from −19 and −23 mV) compared to PLGA NPs (ranging from −25 and −28 mV), owing to the charge-neutral PEG chains residing on the surface of the NP. The encapsulation efficiency (EE%) of the lipophilic CBD reached nearly 100% in all the nanoparticles studied (Table 1). SEM and TEM images of the fabricated PLGA and PLGA-PEG NPs further confirmed their globular morphology and showed a size range falling within that analyzed by DLS (Figure 1).

Based on the characterization results of the developed nanosystems, PEGylated PLGA NPs were selected and used as delivery nanocarriers to overcome the unfavorable physicochemical properties of CBD in the in vitro assays performed in this study.

3.2 | In Vitro Release of CBD From Nanoparticles

The in vitro release of CBD from the PLGA-PEG NPs and PEGylated PLGA NPs was assessed in PBS (pH 7.4 ± 0.1) containing 0.5%

TABLE 1 | Characteristics of blank (drug-free) NPs, CBD-loaded PLGA and PEG-PLGA nanoparticles (values are mean ± SD) ($n = 9$).

| Formulation		CBD (%w/w)	$D_{mean} \pm SD$ (nm)	PdI ± SD	ZP ± SD (mV)	EE ± SD (%)	DL ± SD (%)
Non-PEGylated	Blank	—	259 ± 5	0.141 ± 0.033	−26.0 ± 3.4	—	—
	CBD loaded	10	247 ± 9	0.154 ± 0.047	−25.6 ± 3.2	99.3 ± 0.5	9.9 ± 0.1
		12.5	262 ± 14	0.202 ± 0.026	−27.3 ± 4.3	98.3 ± 1.2	12.1 ± 0.2
		15	260 ± 5	0.147 ± 0.034	−28.4 ± 1.0	99.7 ± 0.7	15.0 ± 0.1
PEGylated	Blank	—	135 ± 5	0.259 ± 0.017	−21.2 ± 1.6	—	—
	CBD loaded	10	138 ± 8	0.242 ± 0.012	−23.0 ± 1.8	97.1 ± 2.2	9.7 ± 0.2
		12.5	155 ± 11	0.245 ± 0.031	−22.5 ± 2.0	99.6 ± 0.2	12.4 ± 0.1
		15	154 ± 7	0.228 ± 0.017	−19.1 ± 1.4	98.9 ± 0.6	14.6 ± 0.1
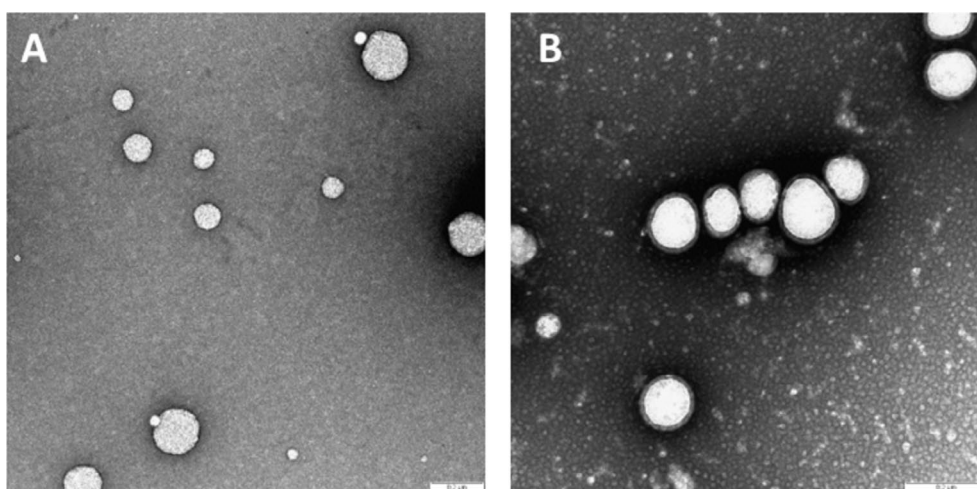
FIGURE 1 | Representative TEM imaging of PLGA (A) and PEG-PLGA (B) nanosystems. Scale bar: 0.2 μm.

(w/v%) Tween 80 at 37.0°C ± 0.5°C. Given the observed partial degradation of CBD under the experimental conditions, evidenced by the appearance of novel chromatographic peaks and a concomitant reduction in free drug concentration (Figures S1 and S2), CBD release was quantified indirectly by assessing the residual drug content within the NPs.

The release profiles of both nanoformulations demonstrated a biphasic pattern, characterized by an initial burst release of approximately 37% of the encapsulated CBD within the first 30 min, followed by a sustained release phase extending over 96 h (Figure 2).

The f_1/f_2 analysis revealed that PLGA and PEG-PLGA NPs exhibited statistically similar release profiles, with $f_1 = 8.2$ (below the 15-threshold) and $f_2 = 57.3$ (above the 50-threshold). Although PLGA NPs showed marginally faster release at some time points, specifically releasing approximately 13% less CBD at the 12, 36, and 48-h time points ($p < 0.05$), the f_1/f_2 results confirm that PEGylation did not significantly alter release kinetics in the nanosystem.
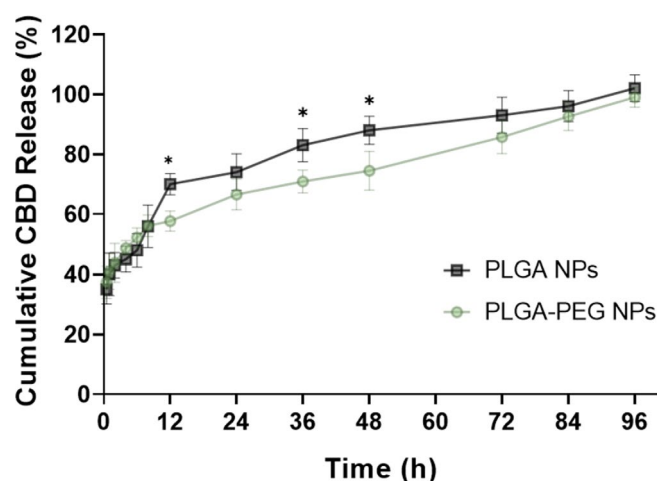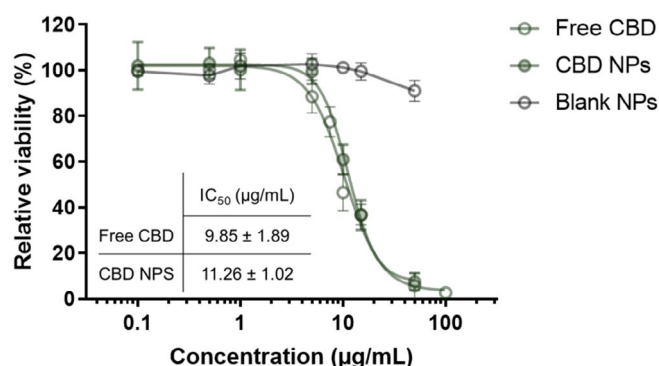

FIGURE 2 | In vitro cumulative release of CBD from nanosystems. CBD release kinetics between PLGA and PLGA-PEG NPs was performed over 96 h in the release medium. Data are represented as the mean ± SD of three independent release assays ($n = 3$), with three replicates in each. Asterisks denote significant differences ($p < 0.05$).

3.3 | Cell Viability Assay

Figure 3 illustrates the in vitro cytotoxic profiles of free CBD, blank (drug-free) NPs, and CBD-loaded PEG-PLGA NPs after 24 h incubation with HepG2 cells. Although the IC50 value was slightly higher for the NPs (11.26 μg/mL; 31.3 μM) compared to the free drug (9.85 μg/mL; 35.8 μM), this difference was not statistically significant. Furthermore, blank NPs exhibited negligible cytotoxicity in this cell line at dilutions corresponding to that of CBD-loaded NPs.

3.4 | Glucose Uptake Assay

To explore the impact of CBD-loaded PEG-PLGA NPs on glucose metabolism, we evaluated the uptake of 2-NBDG by HepG2 cells treated with either free or encapsulated CBD. As demonstrated in Figure 4, cells treated with CBD, whether free or encapsulated, exhibited significantly enhanced 2-NBDG uptake compared to untreated cells ($p < 0.05$), reaching comparable levels to those treated with metformin (50 μg/mL) at CBD concentrations of 1 and 5 μg/mL.

3.5 | Oil Red O Staining

To investigate if encapsulating CBD could prevent cellular lipid accumulation, HepG2 cells were cultured in medium containing sodium palmitate to induce fatty acid overload conditions. An evident increase in cytosolic lipid accumulation was observed in cells exposed to palmitate compared with the control (Figure 5A). Co-incubation of cells with palmitate and CBD, both in free form and encapsulated within NPs, remarkably reduced cellular lipid accumulation (Figure 5B). Furthermore, CBD-loaded NPs, particularly at a concentration of 5 μg/mL, showed a significantly greater effect compared to free drug ($p < 0.05$).

3.6 | Determining Levels of Intracellular Triglyceride and Total Cholesterol and Medium HDL-c

We further investigated the potential of CBD NPs in reducing TG and total cholesterol accumulation in HepG2 cells and elevating HDL-c level in the culture medium. The results are presented in Figure 6. Similar to the findings in the Oil Red O staining experiment, exposure to sodium palmitate (0.35 mM) increased TG (Figure 6A) and total cholesterol (Figure 6B) accumulation in HepG2 cells. However, this effect was notably suppressed by the CBD treatment, especially when delivered via drug-encapsulated NPs, particularly at higher concentrations (5 μg/mL), exhibiting significantly enhanced efficacy compared to the free drug ($p < 0.05$). Likewise, HDL-c levels in the culture medium, reduced by palmitate, were substantially improved by the cannabinoid treatment and nearly fully restored by CBD NPs at a concentration of 5 μg/mL (Figure 6C). These findings demonstrate the significant enhancement of compromised lipid metabolism induced by palmitate in HepG2 cells achieved through CBD-loaded PEG-PLGA NPs.

FIGURE 3 | In vitro viability of HepG2 cells after 24 h of exposure to free CBD, blank (drug-free) NPs and CBD-loaded PEG-PLGA NPs. Data are presented as means ± SD of the relative cell viability (%) from three independent cultures ($n = 3$), with six replicates in each.
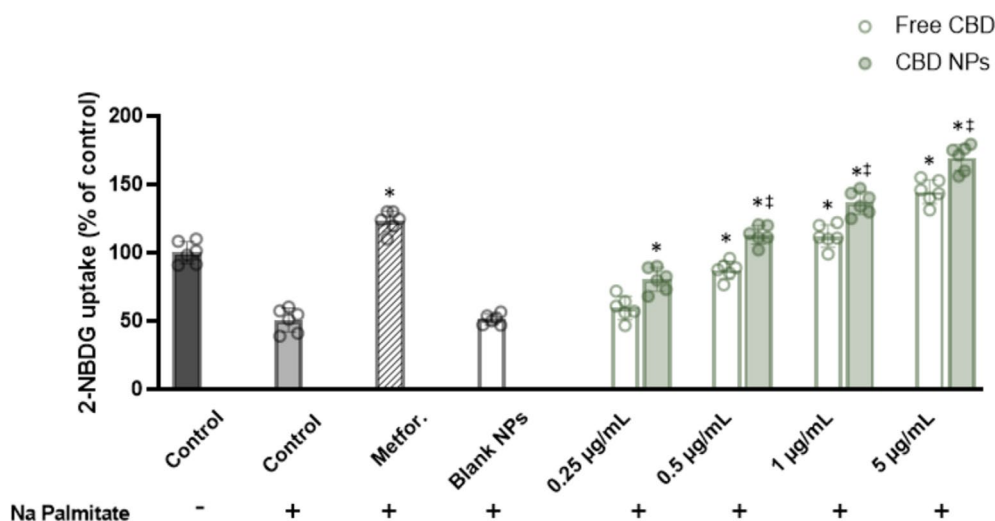

FIGURE 4 | Effects of free CBD and CBD-loaded PEG-PLGA NPs on 2-NBDG uptake in HepG2 cells, following 24-h incubation. Metformin (50 μg/mL) was used as a positive control. Data are presented as means ± SD from six independent experiments ($n = 6$), with triplicates in each. Asterisks denote significant differences ($p < 0.05$): * treated groups compared with control/palmitate group; ‡ free CBD compared with CBD NPs (at the same concentration).
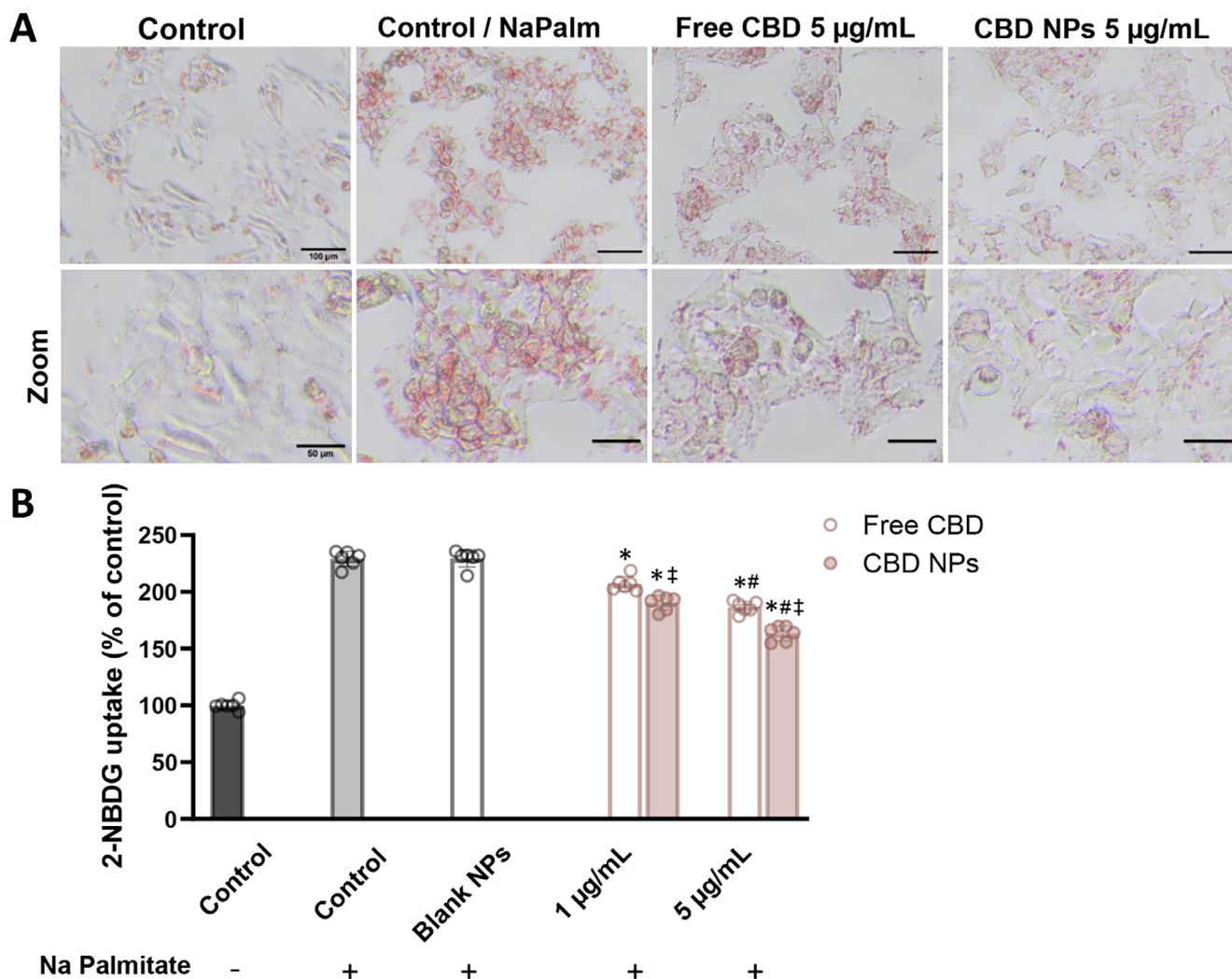
FIGURE 5 | CBD-loaded PEG-PLGA NPs reduce intracellular lipid content in HepG2 cells. Cells were treated with palmitate (0.35 mM) in the absence or presence of free CBD or CBD NPs (1 or 5 μg/mL) for 24 h. (A) HepG2 cells stained with Oil Red O representative images; scale bar: 100 μm; zoom scale bar: 50 μm. (B) Quantitative analysis of total fat levels (absorbance measurement at λ 490 nm). Data are presented as the means ± SD from six independent experiments ($n = 6$), with triplicates in each. Asterisks denote significant differences ($p < 0.05$): * treatments compared with control; # within free CBD groups or within CBD NPs groups; ‡ free CBD compared with CBD NPs (at the same concentration).

3.7 | Gene Expression of Key Metabolic Syndrome Regulators

To delve into the actions of free CBD and CBD-loaded NPs at the molecular level, we assessed the gene expression profiles of key regulators associated with metabolic syndrome in HepG2 cells. Specifically, we examined the expressions of nuclear transcriptional factors such as HNF4α, SREBP-1c, FOXO-1, and PPARγ, along with downstream enzymes involved in glucose and lipid metabolism pathways, including G6Pase, PEPCK, ACC-1, CPT-1, and FAS-1 (Figure 7).

3.7.1 | CBD-NPs Enhances Glucose Uptake by GLUT2

The glucose transporter 2 (GLUT2) facilitates glucose transport in hepatic cells. In the metabolic syndrome conditions, GLUT2 expression was downregulated by 51.3% (Figure 7A), aligning with the reduced glucose uptake induced by palmitate

(Figure 7A). CBD-NPs significantly enhanced GLUT2 expression, up to 2.6-fold at a concentration of 1 μg/mL and 2.8-fold at a concentration of 5 μg/mL, promoting glucose uptake in the presence of the nanoformulations. In contrast, the exposure to free CBD increased GLUT2 expression to a lesser extent than CBD-loaded NPs, by 44.8% at 1 μg/mL and 66.3% at 5 μg/mL.

3.7.2 | CBD-NPs Restores Glucose Metabolism in Hepatic Cells

In the metabolic syndrome condition, the gluconeogenic enzymes implicated in glucose metabolism were overexpressed, up to 2.5-fold for G6Pase and 3-fold for PEPCK (Figure 7A). The free cannabinoid reduced the expression of gluconeogenic enzymes by 20.1%, while CBD-NPs remarkably impaired the transcription of both G6Pase (by 49.8%) and PEPCK (by 38.5%) enzymes, both at a concentration of 5 μg/mL.
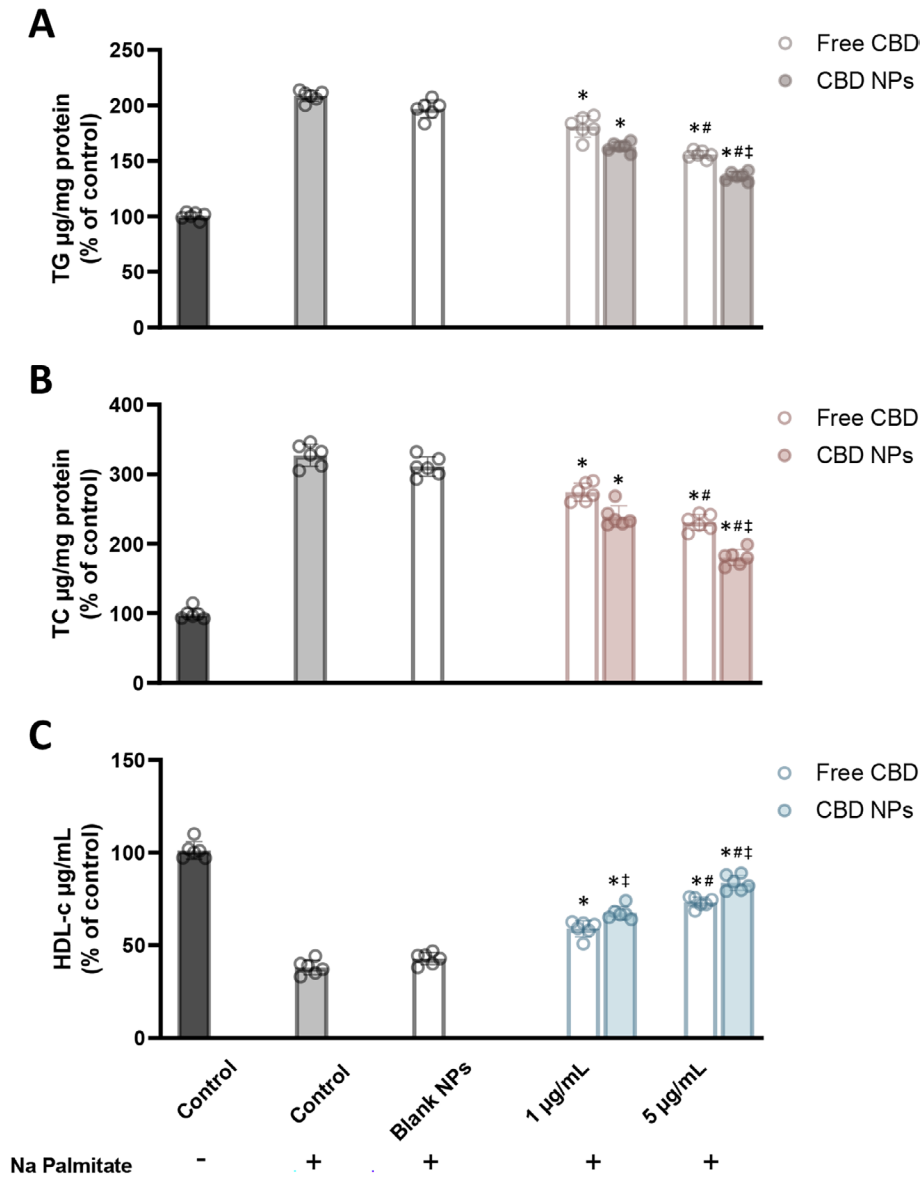
FIGURE 6 | CBD-loaded PEG-PLGA NPs decrease intracellular TG and total cholesterol accumulation and increase HDL-c medium levels in HepG2 cell cultures. (A) TG accumulation in HepG2 cells; (B) Total cholesterol accumulation in HepG2 cells; and (C) HDL-c levels in the medium of HepG2 cells. Data are presented as means ± SD from six independent experiments ($n = 6$), with duplicates in each. Asterisks denote significant differences ($p < 0.05$): * treatments compared with control; # within free CBD groups or within CBD NPs groups; ‡ free CBD compared with CBD NPs (at the same concentration).

3.7.3 | CBD-NPs Regulates Lipid Metabolism

Carnitine palmitoyl transferase I (CPT-1), a key lipolytic enzyme implicated in fatty acid oxidation, exhibited a 47.8% decrease in expression under palmitate treatment (Figure 7B). CBD-NPs treatment significantly increased CPT-1 expression by 68.1% (at 1 μg/mL) and 85.1% (at 5 μg/mL), demonstrating a notably more potent effect than free CBD at the same concentrations. Related to acetyl-coenzyme A carboxylase 1 (ACC-1) and Fatty acid synthase 1 (FAS-1), lipogenic enzymes overexpressed in metabolic syndrome, metformin, free CBD, and CBD-NPs reduced ACC-1 and FAs1 expression by 19.8%, 47.4%–53.4%, and 60.3%–66.8%, respectively (Figure 7B). CBD-NPs restored ACC-1 and FAS1 mRNA expression to control levels at a concentration of 5 μg/mL.

3.7.4 | CBD-NPs Regulates Transcriptional Factors (TFs) Involved in Metabolic Syndrome

The Forkhead box protein O1 (FOXO-1) and the peroxisome proliferator-activated receptor gamma (PPARγ) contribute to the overproduction of gluconeogenic enzymes PEPCK and G6Pase in metabolic syndrome [69]. According to that, in palmitate-stimulated cells FOXO and PPARγ expression increased up to 3-fold for both genes (Figure 7C). CBD loaded NPs reduced FOXO-1 mRNA levels by 55.2% (1 μg/mL) and 64.2% (5 μg/mL), which was more drastic than the reduction observed with free CBD at the same concentrations (43.1% and 46.2%) ($p < 0.001$). PPARγ expression was also restricted under cannabinoid treatment, showing a reduction of 38.1% and 54.2% for free CBD and
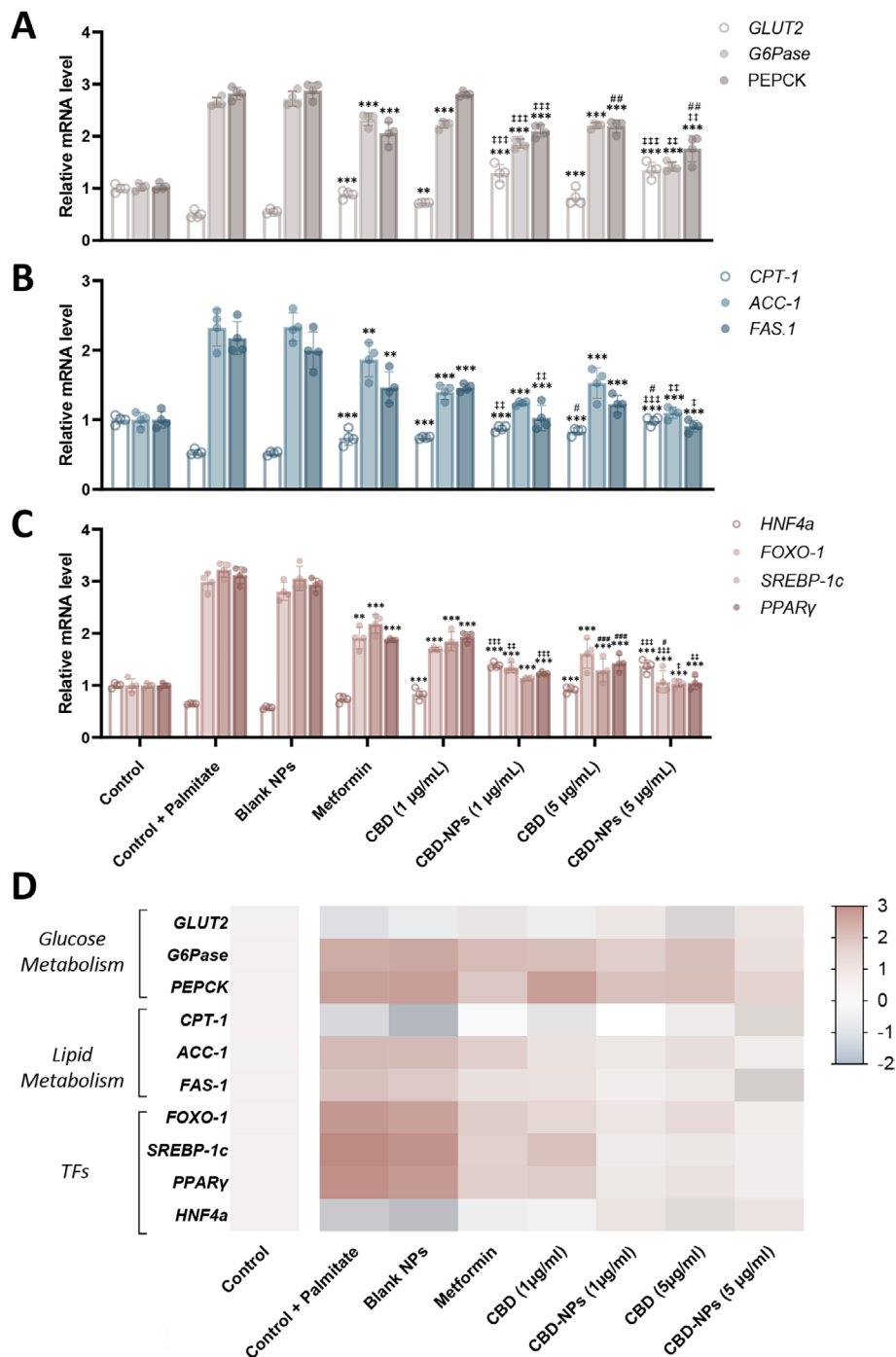
FIGURE 7 | Relative mRNA levels of genes associated with metabolic syndrome in human hepatic cells. Relative expression of genes involved in glucose transport and metabolism (A), lipolysis and lipogenesis (B) and crucial transcription factors (TFs) (C) in metabolic syndrome. Heat map visualizing the normalized gene expression levels of key genes related to metabolic syndrome, highlighting differential expression between control and treated samples (D). Data are presented as means $\pm$ SD from independent experiments ($n = 4$), with duplicates in each. Statistically significant differences in relative mRNA levels between treated groups compared with Control + Palmitate are denoted as $*p < 0.05$, $**p < 0.01$, $***p < 0.001$. Statistically significant differences within free CBD groups or CBD NPs groups are highlighted as $\#p < 0.05$, $\#\#p < 0.01$, $\#\#\#p < 0.001$. Statistically significant differences between free CBD and CBD NPs at the same concentration are indicated as $\ddagger p < 0.05$, $\ddagger\ddagger p < 0.01$, $\ddagger\ddagger\ddagger p < 0.001$.

60.5% and 66.5% for CBD NPs at concentrations of 1 and 5 µg/ mL, respectively.

The Sterol Regulatory Element-Binding Protein 1 (SREBP-1c) induces the expression of genes for de novo fatty acid biosynthesis such as ACC-1 and FAS-1 [70, 71]. In hepatic cells of

the metabolic syndrome model, the expression of SREBP-1c increased up to 3.3-fold (Figure 7C). After cannabinoid treatment, whether free or encapsulated, SREBP-1c mRNA levels were comparable to the control, exhibiting a drastic reduction of 65.2% versus 32.2% (1 µg/mL) and 68.9% versus 50.1% (5 µg/ mL) in the case of CBD-NPs versus free CBD when compared

with palmitate-stimulated cells. Thus, CBD NPs downregulated SREBP-1c and its downstream lipogenic genes ACC-1 and FAS-1.

In metabolic syndrome, both insulin resistance and elevated hepatic fat levels are associated with low expression levels of Hepatocyte Nuclear Factor 4 Alpha (HNF4α) [72]. In palmitate-treated cells, HNF4α mRNA levels were also decreased by 35.5% (Figure 7C). CBD NPs more efficiently counteracted HNF4α suppression than free CBD, resulting in elevated HNF4α relative expression (74.1% for CBD NPs versus 18.2% for free CBD) and inhibiting lipogenesis.

4 | Discussion

In this work, PLGA-based NPs of CBD were developed and characterized, and the impact of CBD encapsulation on its ability to ameliorate palmitate-induced metabolic syndrome lipid accumulation was investigated in vitro in human hepatic cells.

Among the key advantages of PEG-PLGA based nanoparticles used as drug carriers are their ability to overcome biological barriers in the body and target the drug to its site of action. These exceptional properties lead to the enhancement of in vivo pharmacokinetics of the encapsulated cargo, signified by improved bioavailability, reduced clearance, and increased circulation half-time [73]. PEG-PLGA-based NPs can be employed to enhance the solubility of highly lipophilic substances, as in the case of CBD, provide a sustained/controlled drug release profile, and, due to the PEGylation, enhance mucous penetration and prevent opsonization, thus giving stealth particles with prolonged blood half-life [74, 75]. Although non-PEGylated PLGA NPs can be rapidly taken up by components of the mononuclear phagocyte system (MPS) in the liver, mainly Kupffer cells, which are the most numerous cell population of MPS this may block NP delivery to other liver cells [76, 77], and other sites in the body where CBD can exert its pharmacological effects related to the management of metabolic syndrome [30, 33]. Therefore, the hydrophilic neutral coat provided by the PEG chains is expected to prevent non-specific interactions with MPS when NPs arrive at the site of action to release the encapsulated CBD. Furthermore, the exceptional properties of PEG-PLGA NPs render them suitable for drug delivery through various administration routes. Particularly noteworthy is the reduced size of PEGylated NPs (approximately 135–155 nm) compared to unmodified PLGA NPs (approximately 245–265 nm), given that the ideal range for NPs transcytosis in gastrointestinal applications falls between 100 and 200 nm [43], and their hydrophilic neutral surface, known to facilitate effective mucosal penetration, which both are vital advantages for oral administration [78].

In this study, we examined drug release from PLGA and PEG-PLGA NPs. The release pattern of CBD from our nanoparticles exhibited a biphasic behavior characteristic of PLGA-based NPs, closely resembling previously observed results for CBD-loaded PLGA NPs [79]. The initial burst release of CBD is likely due to the rapid diffusion of loosely bound drug molecules on the nanoparticle surface, while the sustained release phase is attributed to the gradual degradation of the polymer matrix via hydrolysis, extending drug release over several days. The similarity in release profiles ($f_1 = 8.2$, $f_2 = 57.3$) between PEGylated and non-PEGylated PLGA NPs suggests that while the hydrophilic PEG barrier appeared to delay CBD diffusion (as evidenced by marginally faster release from non-PEGylated NPs at 12, 36, and 48-h time points), its overall effect on release kinetics was minimal under the tested conditions. Although PBS is a commonly used medium for in vitro drug release studies due to its ability to maintain physiological pH and ionic strength [80, 81], it does not fully replicate the complexity of in vivo environments. Key factors such as protein binding, enzymatic metabolism, and cellular interactions, which can influence the pharmacokinetics and therapeutic efficacy of CBD, are absent in PBS [82]. To more accurately reflect the in vivo behavior of CBD, future studies should consider using serum-based media, tissue-mimicking fluids, or even in vivo models. These approaches would provide a more comprehensive understanding of CBD's release dynamics, stability, and potential therapeutic effects.

CBD possesses low stability and is susceptible to degradation from light exposure and auto-oxidation [83]. Its stability is influenced by several factors, including temperature and solvent (e.g., CBD has lower stability in aqueous solutions compared to ethanol). Furthermore, studies have reported a 10% degradation of CBD under simulated physiological conditions (pH 7.4 and 37°C) [84]. In this work, we observed a similar degradation trend of free CBD under comparable conditions. However, the encapsulation of CBD within NPs is anticipated to shield the drug from external factors, enhancing its stability [85].

The MTT assay was performed to assess the cytotoxicity of CBD and to select the non-toxic concentrations to be used in therapeutic activity experiments. The IC50 value of free CBD (9.9 μg/mL, 31.3 μM) measured in this work was within the range previously reported for HepG2 cells (between 20 and 40 μM after 24 h incubation) [86]. It has been suggested that CBD exerts its cytotoxicity in HepG2 cells through DNA damage [87]. Although the IC50 of the CBD NPs (11.3 μg/mL; 35.8 μM) was marginally higher than that of free CBD, no statistically significant difference was observed between the two treatments.

The HepG2 cell model has been widely employed to study metabolic syndrome-associated hepatic dysfunction due to its ability to recapitulate key metabolic alterations observed in vivo. Previous studies have demonstrated that exposure to high glucose and free fatty acids leads to excessive lipid accumulation, mitochondrial dysfunction, and insulin resistance, resembling the pathophysiology of NAFLD and metabolic syndrome [59, 62]. While HepG2 cells lack some features of primary hepatocytes, such as the full capacity for lipoprotein secretion and xenobiotic metabolism, they remain a valuable tool for evaluating molecular mechanisms underlying metabolic disturbances [88]. Furthermore, their reproducibility, ease of culture, and responsiveness to metabolic stressors make them a suitable model for studying potential therapeutic interventions, including cannabinoids. The use of this model in our study allows for mechanistic insights into how CBD modulates lipid metabolism, which could be further validated in primary hepatocytes or in vivo models [89].

In the glucose uptake experiment, we employed 2-NBDG, a fluorescent-tagged glucose bioprobe, facilitating monitoring of glucose absorption in live cells [63, 90]. Our study revealed a positive correlation between the effect of CBD on glucose utilization and the cannabinoid concentration. Notably, this effect was significantly enhanced by encapsulated cannabinoid. These results highlight the role of PLGA NPs in amplifying CBD′s impact on cellular glucose internalization and, consequently, its metabolism.

In healthy hepatic metabolism, FOXO-1 is typically inhibited by insulin. However, in metabolic syndrome, insulin resistance leads to the activation of FOXO-1 and its associated genes. Notably, elevated FOXO activity results in the upregulation of PPARγ and in the overproduction of gluconeogenic enzymes, such as PEPCK and G6Pase [91]. Our results indicated that after CBD NPs treatment, FOXO-1 and PPARγ mRNA levels were highly suppressed, aligning with the inhibition of gluconeogenic enzymes PEPCK and G6Pase. Consequently, in vitro CBD nanosystems treatment resulted in reduced gluconeogenesis and lowered hyperglycemia.

Moreover, as mentioned above, glucose uptake was enhanced by CBD-loaded NPs, which may be attributed to the overexpression of GLUT2 after NP incubation. GLUT2, the predominant glucose transporter in hepatic cells (accounting for 97% of glucose transport), is essential for glucose absorption in the liver. In the context of metabolic syndrome, reduced GLUT2 expression could adversely affect fat and energy metabolism in the body. Therefore, maintaining an optimal level of GLUT2 is vital for normal glucose uptake in the liver [92]. Thus, the administration of CBD NPs contributed to the restoration of GLUT2 expression, enhancing glucose absorption in human hepatic cells.

Atherogenic dyslipidemia is a notable component of metabolic syndrome. Earlier studies, both in vitro and in vivo, have demonstrated promising outcomes with cannabis oil derivatives, containing CBD and THC, in the management of hypercholesterolemia. These studies showcased a significant reduction in total cholesterol (TC), LDL, and triglycerides (TG), accompanied by a simultaneous increase in HDL when compared to control groups [93, 94]. In our investigation, we also observed the reduction of the lipid parameters (cholesterol and TG) and the increase of HDL-c levels following the treatment of human hepatic cells with the CBD-loaded nanoformulations.

To test the effect of CBD NPs in reducing lipid accumulation, we co-treated the cells with sodium palmitate. It has previously been shown that palmitate, at the same concentration range used in the current study, can induce a substantial deposition of lipids in HepG2 cells, causing steatosis. Palmitate has been found to upregulate the genes responsible for lipogenesis, namely the SREBP-1c pathway, resulting in the incorporation of palmitate into TG in these cells [95]. It can also increase the cholesterol accumulation through the induction of de novo cholesterol biosynthesis [96]. The results of the Oil Red O staining (total lipid accumulation) and TG and cholesterol measurements consistently demonstrated the superiority of the CBD NPs over the free drug in reducing intracellular lipid accumulation.

CBD-loaded NPs effectively inhibited lipogenesis in hepatic cells by reducing the gene expression of SREBP-1c protein, FAS-1, and ACC-1 enzymes. This reduction led to decreased levels of triglycerides and cholesterol and a notable reduction in Oil Red O (ORO)-positive lipid accumulation. Remarkably, this effect was more potent when compared to free cannabidiol at the same concentration. Consistent with these findings, recent studies have reported that cannabidiol treatment positively influences muscular lipid profiles by modulating the expression of fatty acid transporters and inhibiting de novo lipogenesis [31].

In addition, elevated fat storage and the suppression of fatty acid oxidation were observed in the metabolic syndrome model. Our results showed that lipid accumulation, monitored by ORO staining, and CPT-1 expression in palmitate-treated HepG2 cells were higher than in control cells. Interestingly, the nanoformulations led to increased fatty acid oxidation, indicated by elevated CPT-1 expression, and subsequently resulted in reduced lipid storage in hepatic cells when compared to treatment with metformin and free cannabinoids.

The improved therapeutic effect of CBD encapsulated in PEG-PLGA NPs, compared to free CBD, can be attributed to several factors. The nanoparticles provide a sustained release of CBD, which helps maintain consistent therapeutic levels over time, rather than the fluctuations seen with free CBD. In addition, small size particles mean large surface area and saturation solubility, which in turn improve the release rate of CBD [85, 97, 98]. This controlled release profile is critical for achieving optimal therapeutic outcomes, as demonstrated by previous research utilizing similar polymeric nanoparticle systems for drug delivery [99]. This fact could provide a higher concentration in the media, allowing for better CBD absorption. The small size, along with the PEG coating of the nanoparticles, aids in cellular uptake and likely contributes to the stronger therapeutic effect observed in our in vitro experiments. Furthermore, the controlled release from the nanoparticles may also help minimize the risk of cytotoxic effects associated with high doses of free CBD.

5 | Conclusions

In this study, we successfully developed and characterized PEGylated PLGA-based NPs encapsulating CBD and explored their potential for managing metabolic disorders, including those induced by antipsychotic treatments. The CBD-loaded PEGylated PLGA NPs were formulated using the nanoprecipitation technique, resulting in NPs with an optimal size distribution, negative zeta potential, and high encapsulation efficiency. These physicochemical properties contributed to improved NP stability and sustained CBD release, which are critical for therapeutic efficacy. The formulated nanoparticles significantly improved the metabolic effects of CBD in our in vitro metabolic syndrome model of human hepatic cells, as demonstrated by: (i) decreased gluconeogenesis through the downregulation of PPARγ, FOXO-1, PEPCK, and G6Pase, (ii) enhanced glucose uptake and GLUT2 expression, (iii) improved lipid metabolism, with a reduction in cholesterol and triglyceride levels alongside an increase in HDL-c concentration, (iv) decreased intracellular lipid accumulation,

and (v) inhibition of lipogenesis markers (FAS-1 and ACC-1) while promoting fatty acid oxidation (CPT-1). Overall, the encapsulation of CBD in PEGylated PLGA nanoparticles markedly improved the effects of the cannabinoid in our in vitro metabolic syndrome model of human hepatic cells. This enhancement was evidenced by: (i) decreased gluconeogenesis by the downregulation of PPARγ, FOXO-1, PEPCK, and G6Pase, (ii) enhanced glucose uptake and GLUT2 expression, (iii) improved lipid profile by reducing cholesterol and triglyceride levels while increasing HDL-c concentration, (iv) suppressed lipid accumulation, and (v) inhibited lipogenesis (FAS-1 and ACC-1) and promoted fatty acid oxidation (CPT-1). In summary, the PEGylated PLGA nanoparticles effectively potentiated the therapeutic actions of CBD in our model, highlighting their potential as a nanocarrier system for metabolic disorder therapies. These promising findings set the ground for future in vivo studies, further evaluating the therapeutic viability of CBD nanoformulations for mitigating metabolic syndrome-related hepatic dysfunctions.

Author Contributions

All authors contributed to the study conception and design. Material preparation, data collection, and analysis of data were performed by Mazen M. El-Hammadi, Lucía Martín-Navarro, Javier Vázquez-Bourgon, and Lucía Martín-Banderas. The first draft of the manuscript was written by Mazen M. El-Hammadi and Lucía Martín-Navarro; all authors commented on previous versions of the manuscript. All authors read and approved the final manuscript.

Disclosure

Mazen M. El-Hammadi, Lucía Martín-Navarro, Esther Berrocoso, Irene Suárez-Pereira, Josefa Álvarez-Fuentes, Javier Vázquez-Bourgon, and Benedicto Crespo-Facorro declare no conflicts of interest. Lucía Martín-Banderas has received consultant honoraria and research funding from Company GB Sciences.

Conflicts of Interest

The authors declare no conflicts of interest.

Data Availability Statement

The datasets generated and/or analyzed during the current study are available from the corresponding author on reasonable request.

References

1. D. C. Henderson, B. Vincenzi, N. V. Andrea, M. Ulloa, and P. M. Copeland, "Pathophysiological Mechanisms of Increased Cardiometabolic Risk in People With Schizophrenia and Other Severe Mental Illnesses," *Lancet Psychiatry* 2, no. 5 (2015): 452–464, https://doi.org/10.1016/S2215-0366(15)00115-7.

2. J. Vazquez-Bourgon, J. Mayoral-van Son, M. Gomez-Revuelta, et al., "Treatment Discontinuation Impact on Long-Term (10-Year) Weight Gain and Lipid Metabolism in First-Episode Psychosis: Results From the PAFIP-10 Cohort," *International Journal of Neuropsychopharmacology* 24, no. 1 (2021): 1–7, https://doi.org/10.1093/ijnp/pyaa066.

3. A. M. Flores, N. Hosseini-Nassab, K. U. Jarr, et al., "Pro-Efferocytic Nanoparticles Are Specifically Taken Up by Lesional Macrophages and Prevent Atherosclerosis," *Nature Nanotechnology* 15, no. 2 (2020): 154–161, https://doi.org/10.1038/s41565-019-0619-3.

4. M. Di Forti, D. Quattrone, T. P. Freeman, et al., "The Contribution of Cannabis Use to Variation in the Incidence of Psychotic Disorder Across Europe (EU-GEI): A Multicentre Case-Control Study," *Lancet Psychiatry* 6, no. 5 (2019): 427–436, https://doi.org/10.1016/S2215-0366(19)30048-3.

5. E. Setien-Suero, O. Martinez-Garcia, V. O. de la Foz, et al., "Age of Onset of Cannabis Use and Cognitive Function in First-Episode Non-Affective Psychosis Patients: Outcome at Three-Year Follow-Up," *Schizophrenia Research* 201 (2018): 159–166, https://doi.org/10.1016/j.schres.2018.05.036.

6. C. Arango, E. Dragioti, M. Solmi, et al., "Risk and Protective Factors for Mental Disorders Beyond Genetics: An Evidence-Based Atlas," *World Psychiatry* 20, no. 3 (2021): 417–436, https://doi.org/10.1002/wps.20894.

7. H. M. Ihler, T. V. Lagerberg, S. H. Lyngstad, I. Melle, and K. L. Romm, "Exploring the Relationship Between Recency and Frequency of Cannabis Use and Diminished Expression and Apathy as Two Dimensions of Negative Symptoms in First Episode Psychosis. A One-Year Follow-Up Study," *Schizophrenia Research* 236 (2021): 89–96, https://doi.org/10.1016/j.schres.2021.08.004.

8. J. Bruins, G. H. M. Pijnenborg, investigators P, PHAMOUS investigators, E. Visser, and S. Castelein, "The Association of Cannabis Use With Quality of Life and Psychosocial Functioning in Psychosis," *Schizophrenia Research* 228 (2021): 229–234, https://doi.org/10.1016/j.schres.2020.11.059.

9. M. Lahteenvuo, A. Batalla, J. J. Luykx, et al., "Morbidity and Mortality in Schizophrenia With Comorbid Substance Use Disorders," *Acta Psychiatrica Scandinavica* 144, no. 1 (2021): 42–49, https://doi.org/10.1111/acps.13291.

10. N. E. Wade, R. Baca, K. E. Courtney, et al., "Preliminary Evidence for Cannabis and Nicotine Urinary Metabolites as Predictors of Verbal Memory Performance and Learning Among Young Adults," *Journal of the International Neuropsychological Society* 27, no. 6 (2021): 546–558, https://doi.org/10.1017/S1355617721000205.

11. T. Schoeler, N. Petros, M. Di Forti, et al., "Poor Medication Adherence and Risk of Relapse Associated With Continued Cannabis Use in Patients With First-Episode Psychosis: A Prospective Analysis," *Lancet Psychiatry* 4, no. 8 (2017): 627–633, https://doi.org/10.1016/S2215-0366(17)30233-X.

12. J. Bruins, M. G. Pijnenborg, A. A. Bartels-Velthuis, et al., "Cannabis Use in People With Severe Mental Illness: The Association With Physical and Mental Health—A Cohort Study. A Pharmacotherapy Monitoring and Outcome Survey Study," *Journal of Psychopharmacology* 30, no. 4 (2016): 354–362, https://doi.org/10.1177/0269881116631652.

13. J. Vazquez-Bourgon, E. Setien-Suero, F. Pilar-Cuellar, et al., "Effect of Cannabis on Weight and Metabolism in First-Episode Non-Affective Psychosis: Results From a Three-Year Longitudinal Study," *Journal of Psychopharmacology* 33, no. 3 (2019): 284–294, https://doi.org/10.1177/0269881118822173.

14. A. Waterreus, P. Di Prinzio, G. F. Watts, et al., "Metabolic Syndrome in People With a Psychotic Illness: Is Cannabis Protective?," *Psychological Medicine* 46, no. 8 (2016): 1651–1662, https://doi.org/10.1017/S0033291715002883.

15. J. Vazquez-Bourgon, V. Ortiz-Garcia de la Foz, I. Suarez-Pereira, et al., "Cannabis Consumption and Non-Alcoholic Fatty Liver Disease. A Three Years Longitudinal Study in First Episode Non-Affective Psychosis Patients," *Progress in Neuro-Psychopharmacology and Biological Psychiatry* 95 (2019): 109677, https://doi.org/10.1016/j.pnpbp.2019.109677.

16. E. A. Penner, H. Buettner, and M. A. Mittleman, "The Impact of Marijuana Use on Glucose, Insulin, and Insulin Resistance Among US Adults," *American Journal of Medicine* 126, no. 7 (2013): 583–589, https://doi.org/10.1016/j.amjmed.2013.03.002.

17. T. B. Rajavashisth, M. Shaheen, K. C. Norris, et al., "Decreased Prevalence of Diabetes in Marijuana Users: Cross-Sectional Data From the National Health and Nutrition Examination Survey (NHANES) III," *BMJ Open* 2 (2012): e000494, https://doi.org/10.1136/bmjopen-2011-000494.

18. O. Alshaarawy and J. C. Anthony, "Cannabis Smoking and Diabetes Mellitus: Results From Meta-Analysis With Eight Independent Replication Samples," *Epidemiology* 26, no. 4 (2015): 597–600, https://doi.org/10.1097/EDE.0000000000000314.

19. I. Ruiz de Azua, G. Mancini, R. K. Srivastava, et al., "Adipocyte Cannabinoid Receptor CB1 Regulates Energy Homeostasis and Alternatively Activated Macrophages," *Journal of Clinical Investigation* 127, no. 11 (2017): 4148–4162, https://doi.org/10.1172/JCI83626.

20. V. Simon and D. Cota, "Mechanisms in Endocrinology: Endocannabinoids and Metabolism: Past, Present and Future," *European Journal of Endocrinology* 176, no. 6 (2017): R309–R324, https://doi.org/10.1530/EJE-16-1044.

21. C. Lipina, L. M. Vaanholt, A. Davidova, et al., "CB1 Receptor Blockade Counters Age-Induced Insulin Resistance and Metabolic Dysfunction," *Aging Cell* 15, no. 2 (2016): 325–335, https://doi.org/10.1111/acel.12438.

22. W. C. Hsiao, K. S. Shia, Y. T. Wang, et al., "A Novel Peripheral Cannabinoid Receptor 1 Antagonist, BPR0912, Reduces Weight Independently of Food Intake and Modulates Thermogenesis," *Diabetes, Obesity and Metabolism* 17, no. 5 (2015): 495–504, https://doi.org/10.1111/dom.12447.

23. D. A. Argueta and N. V. DiPatrizio, "Peripheral Endocannabinoid Signaling Controls Hyperphagia in Western Diet-Induced Obesity," *Physiology and Behavior* 171 (2017): 32–39, https://doi.org/10.1016/j.physbeh.2016.12.044.

24. D. Teixeira, D. Pestana, A. Faria, C. Calhau, I. Azevedo, and R. Monteiro, "Modulation of Adipocyte Biology by Δ9-Tetrahydrocannabinol," *Obesity* 18, no. 11 (2010): 2077–2085, https://doi.org/10.1038/oby.2010.100.

25. S. M. Labbe, A. Caron, D. Lanfray, et al., "Hypothalamic Control of Brown Adipose Tissue Thermogenesis," *Frontiers in Systems Neuroscience* 9 (2015): 150, https://doi.org/10.3389/fnsys.2015.00150.

26. K. O'Brien, "Cannabidiol (CBD) in Cancer Management," *Cancers* 14, no. 4 (2022): 885, https://doi.org/10.3390/cancers14040885.

27. J. Mlost, M. Bryk, and K. Starowicz, "Cannabidiol for Pain Treatment: Focus on Pharmacology and Mechanism of Action," *International Journal of Molecular Sciences* 21, no. 22 (2020): 8870, https://doi.org/10.3390/ijms21228870.

28. F. Patricio, A. A. Morales-Andrade, A. Patricio-Martinez, et al., "Cannabidiol as a Therapeutic Target: Evidence of Its Neuroprotective and Neuromodulatory Function in Parkinson's Disease," *Frontiers in Pharmacology* 11 (2020): 595635, https://doi.org/10.3389/fphar.2020.595635.

29. C. Silvestri and V. Di Marzo, "The Endocannabinoid System in Energy Homeostasis and the Etiopathology of Metabolic Disorders," *Cell Metabolism* 17, no. 4 (2013): 475–490, https://doi.org/10.1016/j.cmet.2013.03.001.

30. P. Bielawiec, E. Harasim-Symbor, and A. Chabowski, "Phytocannabinoids: Useful Drugs for the Treatment of Obesity? Special Focus on Cannabidiol," *Front Endocrinol* 11 (2020): 114, https://doi.org/10.3389/fendo.2020.00114.

31. P. Bielawiec, S. Dziemitko, K. Konstantynowicz-Nowicka, A. Chabowski, J. Dzięcioł, and E. Harasim-Symbor, "Cannabidiol Improves Muscular Lipid Profile by Affecting the Expression of Fatty Acid Transporters and Inhibiting De Novo Lipogenesis," *Scientific Reports* 13, no. 1 (2023): 3694, https://doi.org/10.1038/s41598-023-30872-w.

32. A. A. Scopinho, F. S. Guimaraes, F. M. Correa, and L. B. Resstel, "Cannabidiol Inhibits the Hyperphagia Induced by Cannabinoid-1 or Serotonin-1A Receptor Agonists," *Pharmacology, Biochemistry, and Behavior* 98, no. 2 (2011): 268–272, https://doi.org/10.1016/j.pbb.2011.01.007.

33. R. G. Pertwee, "The Diverse CB1 and CB2 Receptor Pharmacology of Three Plant Cannabinoids: Delta9-Tetrahydrocannabinol, Cannabidiol and Delta9-Tetrahydrocannabivarin," *British Journal of Pharmacology* 153, no. 2 (2008): 199–215, https://doi.org/10.1038/sj.bjp.0707442.

34. C. Silvestri, E. Pagano, S. Lacroix, et al., "Fish Oil, Cannabidiol and the Gut Microbiota: An Investigation in a Murine Model of Colitis," *Frontiers in Pharmacology* 11 (2020): 585096, https://doi.org/10.3389/fphar.2020.585096.

35. C. Pagano, B. Savarese, L. Coppola, et al., "Cannabinoids in the Modulation of Oxidative Signaling," *International Journal of Molecular Sciences* 24, no. 3 (2023): 2513, https://doi.org/10.3390/ijms24032513.

36. K. Iffland and F. Grotenhermen, "An Update on Safety and Side Effects of Cannabidiol: A Review of Clinical Data and Relevant Animal Studies," *Cannabis and Cannabinoid Research* 2, no. 1 (2017): 139–154, https://doi.org/10.1089/can.2016.0034.

37. L. E. Ewing, C. M. Skinner, C. M. Quick, et al., "Hepatotoxicity of a Cannabidiol-Rich Cannabis Extract in the Mouse Model," *Molecules* 24, no. 9 (2019): 1694, https://doi.org/10.3390/molecules24091694.

38. T. Huang, T. Xu, Y. Wang, et al., "Cannabidiol Inhibits Human Glioma by Induction of Lethal Mitophagy Through Activating TRPV4," *Autophagy* 17, no. 11 (2021): 3592–3606, https://doi.org/10.1080/15548627.2021.1885203.

39. C. J. Lucas, P. Galettis, and J. Schneider, "The Pharmacokinetics and the Pharmacodynamics of Cannabinoids," *British Journal of Clinical Pharmacology* 84, no. 11 (2018): 2477–2482, https://doi.org/10.1111/bcp.13710.

40. V. Franco, P. Gershkovich, E. Perucca, and M. Bialer, "The Interplay Between Liver First-Pass Effect and Lymphatic Absorption of Cannabidiol and Its Implications for Cannabidiol Oral Formulations," *Clinical Pharmacokinetics* 59, no. 12 (2020): 1493–1500, https://doi.org/10.1007/s40262-020-00931-w.

41. T. A. Bhat, S. G. Kalathil, M. L. Goniewicz, A. Hutson, and Y. Thanavala, "Not All Vaping Is the Same: Differential Pulmonary Effects of Vaping Cannabidiol Versus Nicotine," *Thorax* 78, no. 9 (2023): 922–932, https://doi.org/10.1136/thorax-2022-218743.

42. S. Khizar, N. Alrushaid, F. Alam Khan, et al., "Nanocarriers Based Novel and Effective Drug Delivery System," *International Journal of Pharmaceutics* 632 (2023): 122570, https://doi.org/10.1016/j.ijpharm.2022.122570.

43. M. J. Mitchell, M. M. Billingsley, R. M. Haley, M. E. Wechsler, N. A. Peppas, and R. Langer, "Engineering Precision Nanoparticles for Drug Delivery," *Nature Reviews: Drug Discovery* 20, no. 2 (2021): 101–124, https://doi.org/10.1038/s41573-020-0090-8.

44. J. Liu, H. Cabral, and P. Mi, "Nanocarriers Address Intracellular Barriers for Efficient Drug Delivery, Overcoming Drug Resistance, Subcellular Targeting and Controlled Release," *Advanced Drug Delivery Reviews* 207 (2024): 115239, https://doi.org/10.1016/j.addr.2024.115239.

45. M. El-Hammadi and J. L. Arias, "Advanced Engineering Approaches in the Development of PLGA-Based Nanomedicines," in *Handbook of Nanoparticles*, ed. M. Aliofkhazraei (Springer International Publishing, 2015), 1009–1039, https://doi.org/10.1007/978-3-319-13188-7_45-1.

46. M. M. El-Hammadi and J. L. Arias, "Recent Advances in the Surface Functionalization of PLGA-Based Nanomedicines," *Nanomaterials* 12, no. 3 (2022): 354, https://doi.org/10.3390/nano12030354.

47. L. Shi, J. Zhang, M. Zhao, et al., "Effects of Polyethylene Glycol on the Surface of Nanoparticles for Targeted Drug Delivery," *Nanoscale* 13, no. 24 (2021): 10748–10764, https://doi.org/10.1039/d1nr02065j.

48. Y. A. Haggag, A. M. Faheem, M. M. Tambuwala, et al., "Effect of Poly(Ethylene Glycol) Content and Formulation Parameters on Particulate Properties and Intraperitoneal Delivery of Insulin From PLGA Nanoparticles Prepared Using the Double-Emulsion Evaporation Procedure," *Pharmaceutical Development and Technology* 23, no. 4 (2018): 370–381, https://doi.org/10.1080/10837450.2017.1295066.

49. C. M. Vesa, D. C. Zaha, and S. G. Bungau, "Molecular Mechanisms of Metabolic Syndrome," *International Journal of Molecular Sciences* 25, no. 10 (2024): 5452, https://doi.org/10.3390/ijms25105452.

50. R. Loomba, S. L. Friedman, and G. I. Shulman, "Mechanisms and Disease Consequences of Nonalcoholic Fatty Liver Disease," *Cell* 184, no. 10 (2021): 2537–2564, https://doi.org/10.1016/j.cell.2021.04.015.

51. S. H. Shahcheraghi, A. A. A. Aljabali, M. S. Al Zoubi, et al., "Overview of Key Molecular and Pharmacological Targets for Diabetes and Associated Diseases," *Life Sciences* 278 (2021): 119632, https://doi.org/10.1016/j.lfs.2021.119632.

52. L. Martín-Banderas, I. Munoz-Rubio, J. Alvarez-Fuentes, et al., "Engineering of Δ9-Tetrahydrocannabinol Delivery Systems Based on Surface Modified-PLGA Nanoplatforms," *Colloids and Surfaces. B, Biointerfaces* 123 (2014): 114–122, https://doi.org/10.1016/j.colsurfb.2014.09.002.

53. M. Duran-Lobato, I. Munoz-Rubio, M. A. Holgado, et al., "Enhanced Cellular Uptake and Biodistribution of a Synthetic Cannabinoid Loaded in Surface-Modified Poly(Lactic-Co-Glycolic Acid) Nanoparticles," *Journal of Biomedical Nanotechnology* 10, no. 6 (2014): 1068–1079, https://doi.org/10.1166/jbn.2014.1806.

54. L. Martin-Banderas, J. Alvarez-Fuentes, M. Duran-Lobato, et al., "Cannabinoid Derivate-Loaded PLGA Nanocarriers for Oral Administration: Formulation, Characterization, and Cytotoxicity Studies," *International Journal of Nanomedicine* 7 (2012): 5793–5806, https://doi.org/10.2147/IJN.S34633.

55. E. Berrocoso, R. Rey-Brea, M. Fernandez-Arevalo, et al., "Single Oral Dose of Cannabinoid Derivate Loaded PLGA Nanocarriers Relieves Neuropathic Pain for Eleven Days," *Nanomedicine* 13, no. 8 (2017): 2623–2632, https://doi.org/10.1016/j.nano.2017.07.010.

56. J. Alvarez-Fuentes, L. Martin-Banderas, I. Munoz-Rubio, et al., "Development and Validation of an RP-HPLC Method for CB13 Evaluation in Several PLGA Nanoparticle Systems," *Scientific World Journal* 2012 (2012): 737526, https://doi.org/10.1100/2012/737526.

57. R. Gupta, Y. Chen, and H. Xie, "In Vitro Dissolution Considerations Associated With Nano Drug Delivery Systems," *Wiley Interdisciplinary Reviews. Nanomedicine and Nanobiotechnology* 13, no. 6 (2021): e1732, https://doi.org/10.1002/wnan.1732.

58. A. Molinaro, B. Becattini, and G. Solinas, "Insulin Signaling and Glucose Metabolism in Different Hepatoma Cell Lines Deviate From Hepatocyte Physiology Toward a Convergent Aberrant Phenotype," *Scientific Reports* 10, no. 1 (2020): 12031, https://doi.org/10.1038/s41598-020-68721-9.

59. Z. Wang, S. Ge, S. Li, H. Lin, and S. Lin, "Anti-Obesity Effect of Trans-Cinnamic Acid on HepG2 Cells and HFD-Fed Mice," *Food and Chemical Toxicology* 137 (2020): 111148, https://doi.org/10.1016/j.fct.2020.111148.

60. W. Cui, B. Xu, F. Chen, W. Shen, F. Wan, and A. Cheng, "Effects of Grape Peel Phenolics on Lipid Accumulation in Sodium Palmitate-Treated HepG2 Cells," *Journal of Functional Foods* 112 (2024): 105923, https://doi.org/10.1016/j.jff.2023.105923.

61. M. A. Rodriguez-Hernandez, R. Chapresto-Garzon, M. Cadenas, et al., "Differential Effectiveness of Tyrosine Kinase Inhibitors in 2D/3D Culture According to Cell Differentiation, p53 Status and Mitochondrial Respiration in Liver Cancer Cells," *Cell Death and Disease* 11, no. 5 (2020): 339, https://doi.org/10.1038/s41419-020-2558-1.

62. Y. Li, A. T. Sair, W. Zhao, T. Li, and R. H. Liu, "Ferulic Acid Mediates Metabolic Syndrome via the Regulation of Hepatic Glucose and Lipid Metabolisms and the Insulin/IGF-1 Receptor/PI3K/AKT Pathway in Palmitate-Treated HepG2 Cells," *Journal of Agricultural and Food Chemistry* 70, no. 46 (2022): 14706–14717, https://doi.org/10.1021/acs.jafc.2c05676.

63. Q. Zhang, X. F. Hu, M. M. Xin, et al., "Antidiabetic Potential of the Ethyl Acetate Extract of Physalis Alkekengi and Chemical Constituents Identified by HPLC-ESI-QTOF-MS," *Journal of Ethnopharmacology* 225 (2018): 202–210, https://doi.org/10.1016/j.jep.2018.07.007.

64. Y. Mi, D. Tan, Y. He, X. Zhou, Q. Zhou, and S. Ji, "Melatonin Modulates Lipid Metabolism in HepG2 Cells Cultured in High Concentrations of Oleic Acid: AMPK Pathway Activation May Play an Important Role," *Cell Biochemistry and Biophysics* 76, no. 4 (2018): 463–470, https://doi.org/10.1007/s12013-018-0859-0.

65. X. Zhu, H. Yan, M. Xia, et al., "Metformin Attenuates Triglyceride Accumulation in HepG2 Cells Through Decreasing Stearyl-Coenzyme A Desaturase 1 Expression," *Lipids in Health and Disease* 17, no. 1 (2018): 114, https://doi.org/10.1186/s12944-018-0762-0.

66. L. Zhao, X. Guo, O. Wang, et al., "Fructose and Glucose Combined With Free Fatty Acids Induce Metabolic Disorders in HepG2 Cell: A New Model to Study the Impacts of High-Fructose/Sucrose and High-Fat Diets In Vitro," *Molecular Nutrition and Food Research* 60, no. 4 (2016): 909–921, https://doi.org/10.1002/mnfr.201500635.

67. J. Cai, J. Peng, J. Feng, et al., "Antioxidant Hepatic Lipid Metabolism Can Be Promoted by Orally Administered Inorganic Nanoparticles," *Nature Communications* 14, no. 1 (2023): 3643, https://doi.org/10.1038/s41467-023-39423-3.

68. M. M. El-Hammadi, A. V. Delgado, C. Melguizo, et al., "Folic Acid-Decorated and PEGylated PLGA Nanoparticles for Improving the Antitumour Activity of 5-Fluorouracil," *International Journal of Pharmaceutics* 516, no. 1–2 (2017): 61–70, https://doi.org/10.1016/j.ijpharm.2016.11.012.

69. Y. X. Zhu, H. Q. Hu, M. L. Zuo, et al., "Effect of Oxymatrine on Liver Gluconeogenesis Is Associated With the Regulation of PEPCK and G6Pase Expression and AKT Phosphorylation," *Biomedical Reports* 15, no. 1 (2021): 56, https://doi.org/10.3892/br.2021.1432.

70. J. Bates, A. Vijayakumar, S. Ghoshal, et al., "Acetyl-CoA Carboxylase Inhibition Disrupts Metabolic Reprogramming During Hepatic Stellate Cell Activation," *Journal of Hepatology* 73, no. 4 (2020): 896–905, https://doi.org/10.1016/j.jhep.2020.04.037.

71. J. Y. Liu, Y. C. Zhang, L. N. Song, et al., "Nifuroxazide Ameliorates Lipid and Glucose Metabolism in Palmitate-Induced HepG2 Cells," *RSC Advances* 9, no. 67 (2019): 39394–39404, https://doi.org/10.1039/c9ra06527j.

72. R. Zolfaghari, J. A. Bonzo, F. J. Gonzalez, et al., "Hepatocyte Nuclear Factor 4alpha (HNF4alpha) Plays a Controlling Role in Expression of the Retinoic Acid Receptor Beta (RARbeta) Gene in Hepatocytes," *International Journal of Molecular Sciences* 24, no. 10 (2023): 8608, https://doi.org/10.3390/ijms24108608.

73. B. Stella, F. Baratta, C. Della Pepa, S. Arpicco, D. Gastaldi, and F. Dosio, "Cannabinoid Formulations and Delivery Systems: Current and Future Options to Treat Pain," *Drugs* 81, no. 13 (2021): 1513–1557, https://doi.org/10.1007/s40265-021-01579-x.

74. M. M. El-Hammadi, A. L. Small-Howard, M. Fernández-Arévalo, et al., "Development of Enhanced Drug Delivery Vehicles for Three Cannabis-Based Terpenes Using Poly(Lactic-Co-Glycolic Acid) Based Nanoparticles," *Industrial Crops and Products* 164 (2021): 113345, https://doi.org/10.1016/j.indcrop.2021.113345.

75. M. M. El-Hammadi, A. L. Small-Howard, C. Jansen, et al., "Potential Use for Chronic Pain: Poly(Ethylene Glycol)-poly(Lactic-Co-Glycolic Acid) Nanoparticles Enhance the Effects of Cannabis-Based Terpenes on Calcium Influx in TRPV1-Expressing Cells," *International Journal*

of *Pharmaceutics* 616 (2022): 121524, https://doi.org/10.1016/j.ijpharm.2022.121524.

76. J. K. Park, T. Utsumi, Y. E. Seo, et al., "Cellular Distribution of Injected PLGA-Nanoparticles in the Liver," *Nanomedicine* 12, no. 5 (2016): 1365–1374, https://doi.org/10.1016/j.nano.2016.01.013.

77. B. Boltnarova, J. Kubackova, J. Skoda, et al., "PLGA Based Nanospheres as a Potent Macrophage-Specific Drug Delivery System," *Nanomaterials* 11, no. 3 (2021): 749, https://doi.org/10.3390/nano11030749.

78. Q. Xu, L. M. Ensign, N. J. Boylan, et al., "Impact of Surface Polyethylene Glycol (PEG) Density on Biodegradable Nanoparticle Transport in Mucus Ex Vivo and Distribution In Vivo," *ACS Nano* 9, no. 9 (2015): 9217–9227, https://doi.org/10.1021/acsnano.5b03876.

79. A. I. Fraguas-Sanchez, A. I. Torres-Suarez, M. Cohen, et al., "PLGA Nanoparticles for the Intraperitoneal Administration of CBD in the Treatment of Ovarian Cancer: In Vitro and in Ovo Assessment," *Pharmaceutics* 12, no. 5 (2020): 439, https://doi.org/10.3390/pharmaceutics12050439.

80. M. Zamansky, N. Zehavi, A. C. Sintov, and S. Ben-Shabat, "The Fundamental Role of Lipids in Polymeric Nanoparticles: Dermal Delivery and Anti-Inflammatory Activity of Cannabidiol," *Molecules* 28, no. 4 (2023): 1774, https://doi.org/10.3390/molecules28041774.

81. K. P. Alcantara, J. W. T. Malabanan, N. Nalinratana, W. Thitikornpong, P. Rojsitthisak, and P. Rojsitthisak, "Cannabidiol-Loaded Solid Lipid Nanoparticles Ameliorate the Inhibition of Proinflammatory Cytokines and Free Radicals in an In Vitro Inflammation-Induced Cell Model," *International Journal of Molecular Sciences* 25, no. 9 (2024): 4744, https://doi.org/10.3390/ijms25094744.

82. L. Gómez-Lázaro, C. Martín-Sabroso, J. Aparicio-Blanco, and A. I. Torres-Suárez, "Assessment of In Vitro Release Testing Methods for Colloidal Drug Carriers: The Lack of Standardized Protocols," *Pharmaceutics* 16, no. 1 (2024): 103.

83. S. A. Millar, R. F. Maguire, A. S. Yates, and S. E. O'Sullivan, "Towards Better Delivery of Cannabidiol (CBD)," *Pharmaceuticals* 13, no. 9 (2020): 219, https://doi.org/10.3390/ph13090219.

84. A. Schwarzenberg, H. Carpenter, C. Wright, O. Bayazeid, and M. Brokl, "Characterizing the Degradation of Cannabidiol in an e-Liquid Formulation," *Scientific Reports* 12, no. 1 (2022): 20058, https://doi.org/10.1038/s41598-022-23910-6.

85. C. Wang, J. Wang, Y. Sun, et al., "Enhanced Stability and Oral Bioavailability of Cannabidiol in Zein and Whey Protein Composite Nanoparticles by a Modified Anti-Solvent Approach," *Food* 11, no. 3 (2022): 376, https://doi.org/10.3390/foods11030376.

86. F. Shangguan, H. Zhou, N. Ma, et al., "A Novel Mechanism of Cannabidiol in Suppressing Hepatocellular Carcinoma by Inducing GSDME Dependent Pyroptosis," *Frontiers in Cell and Development Biology* 9 (2021): 697832, https://doi.org/10.3389/fcell.2021.697832.

87. C. Russo, F. Ferk, M. Misik, et al., "Low Doses of Widely Consumed Cannabinoids (Cannabidiol and Cannabidivarin) Cause DNA Damage and Chromosomal Aberrations in Human-Derived Cells," *Archives of Toxicology* 93, no. 1 (2019): 179–188, https://doi.org/10.1007/s00204-018-2322-9.

88. Y. M. Li, S. Y. Zhao, H. H. Zhao, B. H. Wang, and S. M. Li, "Procyanidin B2 Alleviates Palmitic Acid-Induced Injury in HepG2 Cells via Endoplasmic Reticulum Stress Pathway," *Evidence-Based Complementary and Alternative Medicine* 2021 (2021): 8920757, https://doi.org/10.1155/2021/8920757.

89. X. Wang, G. Li, C. Guo, et al., "Ethyl 2-[2,3,4-Trimethoxy-6-(1-Octanoyl)phenyl] Acetate (TMPA) Ameliorates Lipid Accumulation by Disturbing the Combination of LKB1 With Nur77 and Activating the AMPK Pathway in HepG2 Cells and Mice Primary Hepatocytes," *Diabetes, Metabolism, Syndrome and Obesity* 14 (2021): 4165–4177, https://doi.org/10.2147/DMSO.S321246.

90. S. Odeyemi and J. Dewar, "In Vitro Antidiabetic Activity Affecting Glucose Uptake in HepG2 Cells Following Their Exposure to Extracts of Lauridia tetragona (L.f.) R.H. Archer," *PRO* 8, no. 1 (2020): 33.

91. B. Jiang, L. Le, W. Zhai, et al., "Protective Effects of Marein on High Glucose-Induced Glucose Metabolic Disorder in HepG2 Cells," *Phytomedicine* 23, no. 9 (2016): 891–900, https://doi.org/10.1016/j.phymed.2016.05.004.

92. B. Sun, H. Chen, J. Xue, P. Li, and X. Fu, "The Role of GLUT2 in Glucose Metabolism in Multiple Organs and Tissues," *Molecular Biology Reports* 50, no. 8 (2023): 6963–6974, https://doi.org/10.1007/s11033-023-08535-w.

93. W. Huang, Z. Zeng, Y. Lang, et al., "Cannabis Seed Oil Alleviates Experimental Atherosclerosis by Ameliorating Vascular Inflammation in Apolipoprotein-E-Deficient Mice," *Journal of Agricultural and Food Chemistry* 69, no. 32 (2021): 9102–9110, https://doi.org/10.1021/acs.jafc.0c07251.

94. T. Assa-Glazer, J. Gorelick, N. Sela, A. Nyska, N. Bernstein, and Z. Madar, "Cannabis Extracts Affected Metabolic Syndrome Parameters in Mice Fed High-Fat/Cholesterol Diet," *Cannabis and Cannabinoid Research* 5, no. 3 (2020): 202–214, https://doi.org/10.1089/can.2020.0013.

95. J. F. Liu, Y. Ma, Y. Wang, Z. Y. du, J. K. Shen, and H. L. Peng, "Reduction of Lipid Accumulation in HepG2 Cells by Luteolin Is Associated With Activation of AMPK and Mitigation of Oxidative Stress," *Phytotherapy Research* 25, no. 4 (2011): 588–596, https://doi.org/10.1002/ptr.3305.

96. A. Bashiri, D. Nesan, G. Tavallaee, et al., "Cellular Cholesterol Accumulation Modulates High Fat High Sucrose (HFHS) Diet-Induced ER Stress and Hepatic Inflammasome Activation in the Development of Non-Alcoholic Steatohepatitis," *Biochimica et Biophysica Acta* 1861, no. 7 (2016): 594–605, https://doi.org/10.1016/j.bbalip.2016.04.005.

97. L. Grifoni, G. Vanti, R. Donato, C. Sacco, and A. R. Bilia, "Promising Nanocarriers to Enhance Solubility and Bioavailability of Cannabidiol for a Plethora of Therapeutic Opportunities," *Molecules* 27, no. 18 (2022): 6070, https://doi.org/10.3390/molecules27186070.

98. E. R. Lazzarotto Rebelatto, G. S. Rauber, and T. Caon, "An Update of Nano-Based Drug Delivery Systems for Cannabinoids: Biopharmaceutical Aspects & Therapeutic Applications," *International Journal of Pharmaceutics* 635 (2023): 122727, https://doi.org/10.1016/j.ijpharm.2023.122727.

99. P. Zhang, Y. Liu, G. Feng, et al., "Controlled Interfacial Polymer Self-Assembly Coordinates Ultrahigh Drug Loading and Zero-Order Release in Particles Prepared under Continuous Flow," *Advanced materials letters* 35, no. 22 (2023): e2211254, https://doi.org/10.1002/adma.202211254.

Supporting Information

Additional supporting information can be found online in the Supporting Information section.